

Cite this: *Dalton Trans.*, 2013, **42**, 6149

Cyclen derivatives with two *trans*-methylnitrophenolic pendant arms: a structural study of their copper(II) and zinc(II) complexes†

Catarina V. Esteves,^a Luís M. P. Lima,^a Pedro Mateus,^a Rita Delgado,^{*a} Paula Brandão^b and Vítor Félix^c

Two new cyclen derivatives, H₂do2nph and H₂cb-do2nph, containing two *trans*-2-methyl-4-nitrophenol pendant arms and the latter including also an ethylene cross-bridge, were prepared in good yields using the bisaminal synthetic route. The two ligands were studied comparatively regarding their metal complexation behaviour. The copper(II) and zinc(II) complexes of H₂do2nph and H₂cb-do2nph were studied in dimethylsulfoxide–water (9 : 1 v/v) solution by a range of spectroscopic techniques. Copper(II) complexes were also studied in solid state by X-ray single crystal diffraction. These studies showed that the copper(II) and zinc(II) complexes of H₂do2nph exhibited a distorted square pyramidal coordination environment with the four nitrogen atoms of the cyclen ring defining the basal plane, and that one of the nitrophenolate arms did not coordinate to the metal, independently of its protonation state. On the other hand, depending on the protonation state of one of the nitrophenolic arms, the cross-bridged derivative forms copper(II) complexes with distorted square pyramidal or octahedral geometries with one or two arms coordinated to the metal centre, respectively. In the complex with distorted octahedral geometry, the two phenolic oxygen atoms are coordinated to the metal centre in a *cis*-fashion. Acid-assisted dissociation assays in 1 mol dm⁻³ HCl DMSO–H₂O (9 : 1 v/v) solution at 298.2 K allowed one to determine the half-life of both copper(II) complexes, which is lower for the derivative without a cross-bridge as expected, while for the other one it is quite high and in line with similar cross-bridged cyclen derivatives from the literature.

Received 5th October 2012,
Accepted 14th December 2012

DOI: 10.1039/c2dt32363j

www.rsc.org/dalton

Introduction

Macrocyclic ligands obtained by N-functionalization of cyclen (1,4,7,10-tetraazacyclododecane) continue to be especially interesting due to their ability to form very stable complexes with a range of important metal cations.¹ Between several possible applications, the development of new cyclen

derivatives has recently been particularly driven by the need to find better ligands to chelate cations with potential use in medical imaging and therapy,² such as for magnetic resonance imaging (MRI),³ for diagnosis by positron emission tomography (PET) and single-photon emission computed tomography (SPECT),^{4,5} or for α - and β -radiotherapy.⁵ Among transition metals and related ones, possible isotopes for radiotherapy are ⁶⁷Cu, while important isotopes for imaging are ⁶⁴Cu and ⁶⁸Ga for PET or ⁶⁷Ga for SPECT.^{4–6}

To be suitable for medical applications, complexes of relevant isotopes must exhibit a range of chemical properties such as high thermodynamic stability, high kinetic inertness, fast and mild complex formation, appropriate pharmacokinetics, and preferably the possibility of coupling with targeting biomolecules.^{1,2,4–6} Stable copper(II) complexes of cyclen derivatives are usually 5- or 6-coordinate in square pyramidal, distorted octahedral or tetragonal preferred geometries. This means that cyclen should be appended with at least one or two coordinating arms to fulfil the coordination demand of this cation. Furthermore, the presence of an ethylene bridge between opposite nitrogen atoms has demonstrated the yield

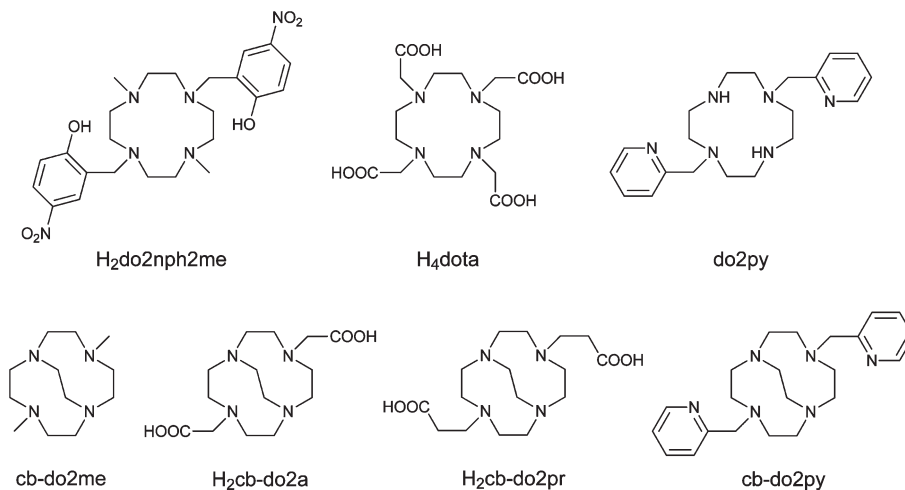
^aInstituto de Tecnologia Química e Biológica, Universidade Nova de Lisboa, Av. da República, 2780-157 Oeiras, Portugal. E-mail: delgado@itqb.unl.pt;

Fax: (+351) 21 441 12 77

^bDepartamento de Química, CICECO, Universidade de Aveiro, 3810-193 Aveiro, Portugal

^cDepartamento de Química, CICECO, and Secção Autónoma de Ciências da Saúde, Universidade de Aveiro, 3810-193 Aveiro, Portugal

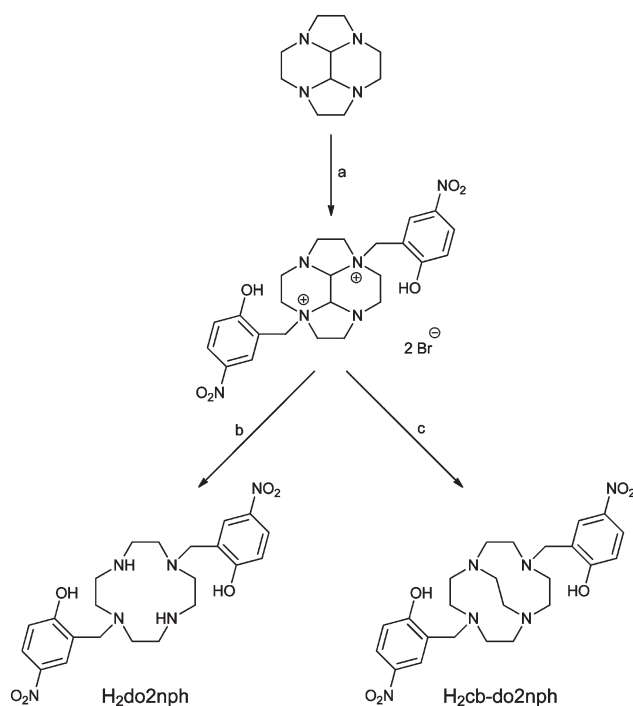
†Electronic supplementary information (ESI) available: X-band EPR spectra of the copper(II) complexes and the corresponding simulated ones; ¹H and ¹³C NMR spectra of the zinc(II) complexes; time course of the dissociation of the copper(II) complexes; ¹H, ¹³C and 2-D NMR spectra of the compounds and their mass spectra. CCDC 904673–904676 for [H₄do2nph](ClO₄)₂·H₂O; [H₂cb-do2nph]·1.5H₂O; [Cu(do2nph)][Cu(Hdo2nph)]ClO₄·3H₂O; [Cu(cb-do2nph)]·H₂O respectively. For ESI and crystallographic data in CIF or other electronic format see DOI: 10.1039/c2dt32363j



Scheme 1 Cyclen derivatives mentioned in this work.

of particularly inert complexes.^{4–6} The choice of useful pendant arms has traditionally been focused on carboxylic and derived moieties although a variety of other substituents were reported, such as phosphonic and aminic among others. Phenolic functions have been rarely appended on cyclen,^{7,8} while they are well known for presenting good coordination ability for copper(II) and also for harder Lewis acid cations such as trivalent transition and lanthanide metals.⁹ Indeed, phenolates have been successfully used by Kimura *et al.* on other macrocyclic skeletons such as cyclam (1,4,8,11-tetraazacyclotetradecane) and 1,5,9-triazacyclododecane in the form of a substituent of the macrocyclic framework.^{10–15} On the other hand, Moore *et al.*^{16,17} and Wieghardt *et al.*^{18,19} used methylphenolic arms N-appended on tacn (1,4,7-triazacyclononane) to study complexes of trivalent metal ions such as gallium(III) and iron(III).

With the above features in mind, we set out to develop a range of new macrocyclic ligands containing methylphenolic pendant arms in their structure, in order to take advantage of their coordination ability for copper(II) and foreseeably also for gallium(III). Our initial approach was focused on cyclen derivatives with complexation properties potentially suitable for yielding octahedral metal coordination environments. Scheme 1 represents the selected literature cyclen derivatives relevant for copper(II) complexation and mentioned along this work. We have developed two new cyclen derivatives, H₂do2nph and H₂cb-do2nph (Scheme 2), both containing two opposite 2-methyl-4-nitrophenol pendant arms and one of them including also an ethylene cross-bridge, in search for enhanced coordination ability towards copper(II). The cross-bridged compound, H₂cb-do2nph, was studied comparatively with the other one, H₂do2nph, regarding their complexation behaviour. Copper(II) and zinc(II) complexes were studied in solution and in solid state by a range of spectroscopic techniques and X-ray single crystal diffraction. The obtained results allowed us to make a detailed analysis of the



Scheme 2 Synthetic procedures used to obtain the compounds H₂do2nph and H₂cb-do2nph. (a) 2-(Bromomethyl)-4-nitrophenol, MeCN, r.t., 8 days; (b) N₂H₄–H₂O, reflux, 2 h; (c) NaBH₄, EtOH–H₂O (9 : 1), r.t., 8 days.

coordination environments adopted in the complexes of both ligands, correlating the solution structures with the ones observed in solid state. The kinetic inertness of both copper(II) complexes was also analysed in acid-assisted dissociation assays, while determination of thermodynamic stability constants for the complexes in solution was hampered by the very low overall solubility of the compounds in any feasible water-containing media. Nonetheless, it is known that, for medical applications, the kinetic inertness of metal complexes is more relevant than their thermodynamic stability.

Results and discussion

Syntheses of the compounds

The compounds $H_2do2nph$ and $H_2cb-do2nph$ were prepared from cyclen-glyoxal according to previously reported routes as shown in Scheme 2. Bisquaternarization of cyclen-glyoxal²⁰ with two equivalents of 2-(bromomethyl)-4-nitrophenol produced the diammonium salt in nearly quantitative yield. From this, $H_2do2nph$ and $H_2cb-do2nph$ were obtained in very good yields, the former by deprotection with hydrazine monohydrate,²¹ and the latter after reduction with sodium borohydride in ethanol/water.²² Both compounds proved to be only sparingly soluble in water and almost insoluble in any other solvent except DMSO, thus limiting significantly possible studies of their chemical properties. For that reason, most solutions of the compounds and their complexes prepared throughout this work used either neat DMSO or a DMSO-water mixture.

Single crystal X-ray studies

Structures of the compounds. The crystal structure of $(H_4do2nph)(ClO_4)_2 \cdot 2H_2O$ salt was built up from an asymmetric unit composed of one $(H_4do2nph)^{2+}$ cation and two ClO_4^- counterions and two crystallisation water molecules. A water molecule is disordered over two positions. The ORTEP diagram of $(H_4do2nph)^{2+}$ presented in Fig. 1 with the labelling scheme adopted shows the secondary nitrogen atoms and the phenol groups protonated as revealed by the last difference Fourier maps calculated along the structure refinement. The $N \cdots O$ and $O \cdots O$ intermolecular distances found in the crystal lattice are consistent with the existence of a 1-D dimensional network of $N-H \cdots O$ and $O-H \cdots O$ hydrogen bonding interactions between $(H_4do2nph)^{2+}$ cations, water crystallisation molecules and ClO_4^- anions. The hydrogen atoms of the disordered water molecule were not considered in this analysis (see below). In addition, the macrocyclic conformation is stabilised by intramolecular bonding interactions including multiple $N-H \cdots N$ hydrogen bonds with $N \cdots N$ distances ranging from 2.834(2) to 2.966(3) Å and a single $N-H \cdots O$ hydrogen bond

with a $N \cdots O$ distance of 3.335(2) Å. These weak and cooperative hydrogen bonds are shown in the right view of Fig. 1.

This structure is rather similar to that found for the related compound containing two additional *N*-methyl pendant arms in the protonation form $(H_3do2nph2me)Br$ (see Scheme 1 for the molecular representation of the compound). In this case the protonations occur at the two cyclen amines bound to the appended methylnitrophenolic groups and at only one of the nitrophenolic groups.²³ The cyclen ring adopts the usual [3333] conformation as in $(H_4do2nph)^{2+}$, however with *trans* $N \cdots N$ distances larger for the reported $(H_3do2nph2me)Br$ (4.37 Å between the protonated amines and 3.88 Å between the methylated amines).

The asymmetric unit of the $H_2cb-do2nph$ is composed of one zwitterionic macrocycle (with one protonated amine in the ring and one of the phenolic groups deprotonated) and two water crystallisation molecules, one with occupancy of 50%. In addition an ethylene linkage in the macrocyclic backbone is disordered over two positions with different occupations as described in the Experimental section. The molecular structure defined by a disordered component is shown in Fig. 2 together with the atomic notation scheme adopted. The single phenol interacts with a crystallisation water molecule through a hydrogen bond with $O \cdots O$ distances of 2.680(11) and $O-H \cdots O$ angles of 124°.

The steric constraints imposed by the ethylene cross-bridge influences the cavity size of $H_2cb-do2nph$ leading to $N \cdots N$ intramolecular distances gathered in Table 1, together with those calculated for $H_2do2nph^{2+}$. However, the $N \cdots N$ distances exhibited by $H_2cb-do2nph$, varying between 2.779(3) and 3.570(3) Å, allow the protonation of a single nitrogen donor of the macrocycle. Furthermore, this proton is stabilised by three intramolecular $N-H \cdots N$ hydrogen bonds with $H \cdots N$ distances of 1.81(5), 2.27(4) and 2.35(5) Å established with N(7), N(1) and N(10) atoms, respectively.

Structures of copper(II) complexes of $H_2do2nph$ and $H_2cb-do2nph$. Selected bond distances and angles in coordination spheres of the copper(II) complexes of $H_2do2nph$ and $H_2cb-do2nph$ are given in Table 2. The asymmetric unit of the

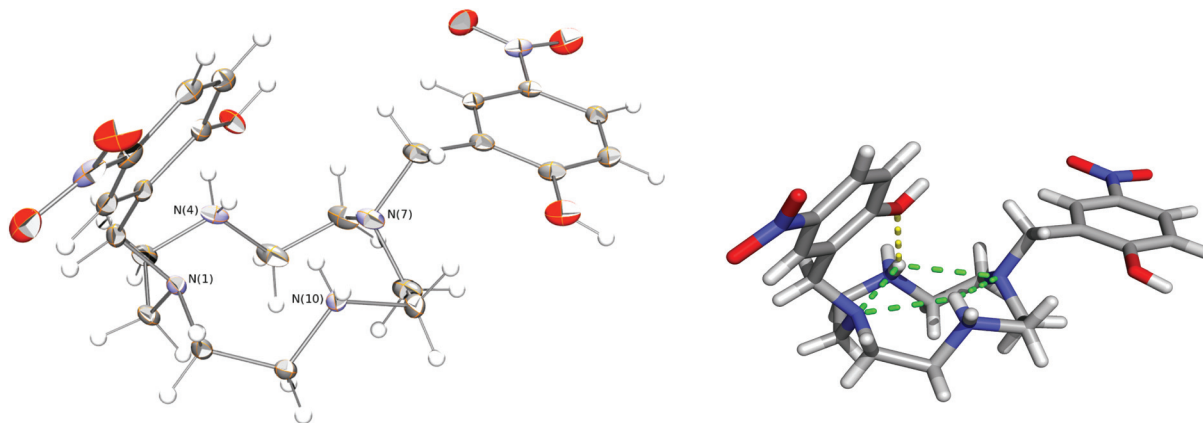


Fig. 1 Structural features of $(H_4do2nph)^{2+}$: ORTEP diagram with thermal ellipsoids drawn at 30% probability level (left view) and the macrocyclic conformation (right view) stabilised by multiple $N-H \cdots N$ and $N-H \cdots O$ hydrogen bonds.

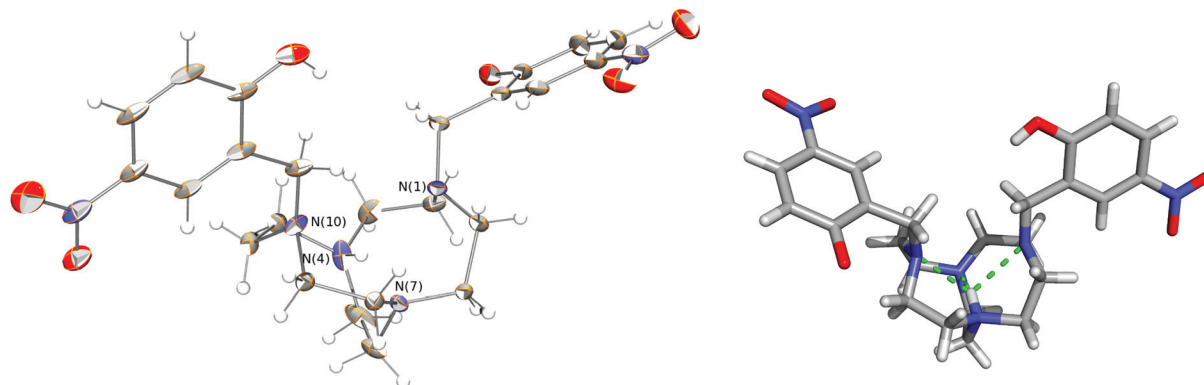


Fig. 2 Perspective views of $\text{H}_2\text{cb-do2nph}$: ORTEP diagram with the labelling scheme adopted for the nitrogen donors and thermal ellipsoids represented at 30% probability level (left) and the macrocyclic conformation stabilised by three $\text{N-H}\cdots\text{N}$ hydrogen bonds drawn as green dashed lines (right). The disordered $-\text{NCH}_2\text{CH}_2\text{N}-$ linkage is shown in a single position for clarity.

Table 1 Intramolecular $\text{N}\cdots\text{N}$ distances (\AA) on the macrocyclic backbone of $(\text{H}_4\text{do2nph})^{2+}$ and $\text{H}_2\text{cb-do2nph}$

Ligand	$(\text{H}_4\text{do2nph})^{2+}$	$\text{H}_2\text{cb-do2nph}$
$\text{N}(1)\cdots\text{N}(4)$	2.834(2)	2.779(3)
$\text{N}(1)\cdots\text{N}(7)$	3.990(2)	2.868(3)
$\text{N}(1)\cdots\text{N}(10)$	2.883(2)	3.570(3)
$\text{N}(4)\cdots\text{N}(7)$	2.966(3)	2.575(3)
$\text{N}(4)\cdots\text{N}(10)$	4.177(2)	2.807(3)
$\text{N}(7)\cdots\text{N}(10)$	2.874(2)	2.779(3)

Table 2 Selected bond distances (\AA) and angles ($^\circ$) in the copper(II) coordination spheres of the complexes of $\text{H}_2\text{do2nph}$ and $\text{H}_2\text{cb-do2nph}$

Complex	$[\text{Cu}(\text{do2nph})]$	$[\text{Cu}(\text{Hdo2nph})]^+$	$[\text{Cu}(\text{cb-do2nph})]$
Bond lengths/ \AA			
$\text{Cu-N}(1)$	2.035(6)	2.027(6)	2.003(4)
$\text{Cu-N}(4)$	2.028(6)	2.015(6)	2.070(4)
$\text{Cu-N}(7)$	2.025(5)	2.028(5)	2.010(4)
$\text{Cu-N}(10)$	2.034(6)	2.027(6)	2.302(4)
$\text{Cu-O}(23)$	2.079(4)	2.086(4)	—
$\text{Cu-O}(25)$	—	—	1.963(4)
$\text{Cu-O}(36)$	—	—	2.343(3)
Bond angles/ $^\circ$			
$\text{N}(7)\text{-Cu-N}(1)$	153.5(2)	154.9(2)	166.77(14)
$\text{N}(4)\text{-Cu-N}(10)$	147.9(2)	146.8(2)	78.26(14)
$\text{N}(1)\text{-Cu-N}(10)$	86.5(3)	86.3(2)	81.55(14)
$\text{N}(4)\text{-Cu-N}(1)$	86.4(2)	86.3(2)	87.90(16)
$\text{N}(7)\text{-Cu-N}(4)$	86.5(2)	87.2(2)	86.00(16)
$\text{N}(7)\text{-Cu-N}(10)$	86.1(2)	85.9(2)	85.71(14)
$\text{O}(25)\text{-Cu-N}(4)$	—	—	177.91(17)
$\text{N}(10)\text{-Cu-O}(36)$	—	—	170.34(12)
$\text{O}(25)\text{-Cu-O}(36)$	—	—	87.64(14)
$\text{N-Cu-O}_{\text{cis-angles, range}}$	95.4(2)– 111.06(19)	94.9(2)– 110.2(2)	87.65(12)– 104.53(13)

complex of $\text{H}_2\text{do2nph}$ contains two copper(II) species with different net charges, $[\text{Cu}(\text{do2nph})]$ and $[\text{Cu}(\text{Hdo2nph})]^+$, one disordered ClO_4^- counterion and three crystallisation water molecules, which is consistent with the molecular formula $[\text{Cu}(\text{do2nph})][\text{Cu}(\text{Hdo2nph})]\text{ClO}_4\cdot 3\text{H}_2\text{O}$. In the complex $[\text{Cu}(\text{do2nph})]$, the two phenolic functional groups are

deprotonated while in the $[\text{Cu}(\text{Hdo2nph})]$ complex a single phenolic group is protonated, as can be seen from their molecular structures presented in Fig. 3. Both complexes exhibit distorted square pyramidal coordination environments with the four nitrogen atoms of the cyclen ring defining the basal plane. The copper centre is positioned above the N_4 coordination plane by 0.513(3) \AA for $[\text{Cu}(\text{do2nph})]$ and 0.510(3) \AA for $[\text{Cu}(\text{Hdo2nph})]^+$, pointing towards the apical oxygen atom from the coordinated 2-methyl-4-nitrophenol arm. Indeed, both complexes exhibit a Cu-O apical oxygen distance, 2.079(4) \AA in $[\text{Cu}(\text{do2nph})]$ and 2.086(4) in $[\text{Cu}(\text{Hdo2nph})]^+$, shorter than the corresponding distance between the oxygen and the basal plane of 2.577(5) and 2.570(5) \AA . The two complexes also have equivalent equatorial Cu-N bond distances (see Table 2). Furthermore, the trigonal distortion was calculated for both complexes using the index structural parameter (τ) as previously defined by Addison *et al.*²⁴ The τ parameter assumes values of 0 and 1 for ideal square pyramidal and trigonal bipyramidal geometries, respectively. The τ values of 0.09 for $[\text{Cu}(\text{do2nph})]$ and 0.13 for $[\text{Cu}(\text{Hdo2nph})]^+$ are entirely consistent with a distorted square pyramidal coordination sphere.

The structures of these two copper(II) complexes compare well with those of the related ligand, $[\text{Cu}(\text{Hdo2nph2me})](\text{ClO}_4)$,⁸ and of cyclen, $[\text{Cu}(\text{cyclen})(\text{NO}_3)]\text{NO}_3$.²⁵ These four structures are however in contrast with those of copper(II) complexes of several cyclen derivatives where instead the copper centre tends to exhibit hexacoordinated environments, like in $[\text{Cu}(\text{H}_2\text{dota})]$,^{26,27} where the copper adopts a distorted octahedral geometry, or in $[\text{Cu}(\text{do2py})]^{2+}$, which is in a distorted triangular prismatic geometry.²⁸

The crystal structure is stabilised by a complex 3-D network of $\text{N-H}\cdots\text{O}$ and $\text{O-H}\cdots\text{O}$ hydrogen bonds in which molecules of $[\text{Cu}(\text{Hdo2nph})]^+$ and $[\text{Cu}(\text{do2nph})]$ are assembled through the NO_2 phenol substituents by water bridges composed of three water molecules.

The molecular structure of $[\text{Cu}(\text{cb-do2nph})]$ is shown in Fig. 4 with the relevant atomic notation scheme adopted. The complex displays a distorted octahedral geometry with two phenolic oxygen atoms coordinated to the metal centre in a

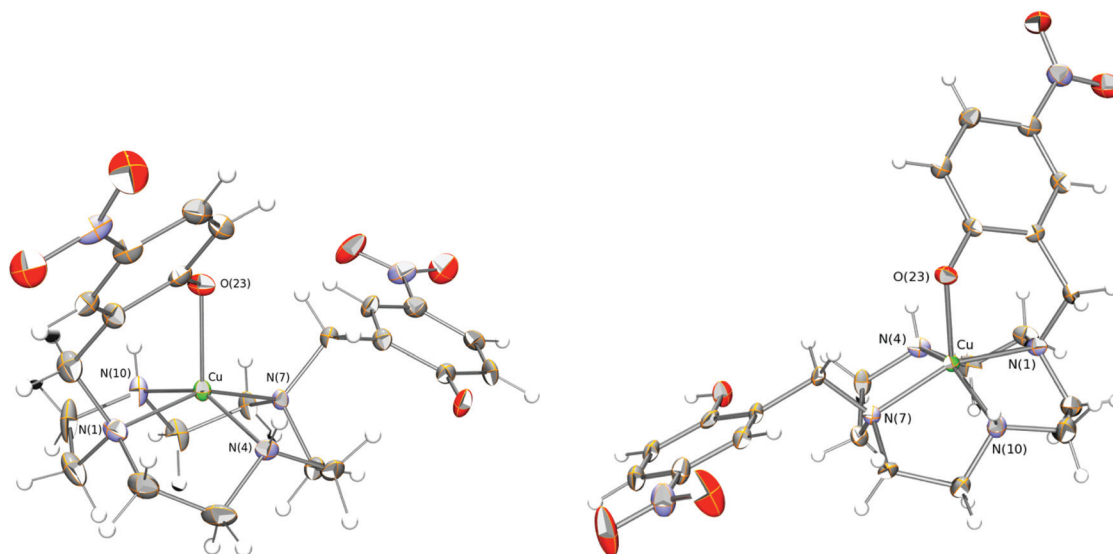


Fig. 3 ORTEP views of $[\text{Cu}(\text{Hdo2nph})]^+$ (left) and $[\text{Cu}(\text{do2nph})]$ (right) with the atomic labelling scheme and thermal ellipsoids drawn at the 50% probability level.

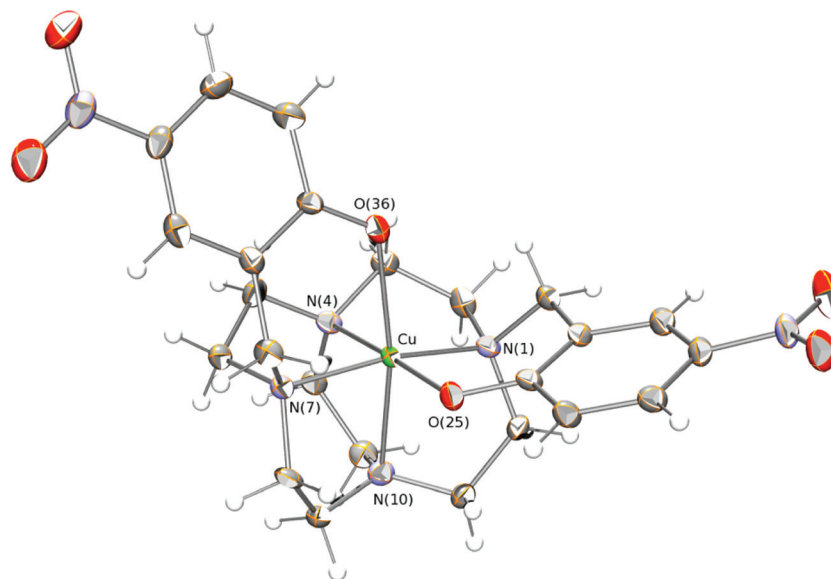


Fig. 4 ORTEP view of $[\text{Cu}(\text{cb-do2nph})]$ showing thermal ellipsoids at the 50% probability level and the relevant atomic labelling scheme adopted.

cis-fashion giving an O–Cu–O angle of $87.64(14)^\circ$. The atoms O(36) and N(10) occupy the apical positions with a N–Cu–O angle of $170.34(12)^\circ$, and Cu–O(36) and Cu–N(10) distances of $2.343(3)$ and $2.302(4)$ Å, respectively. These distances are longer than the remaining four coordination distances ranging between $1.963(4)$ and $2.070(4)$ Å in agreement with the Jahn–Teller effect. The Cu–N equatorial distances compare well with those reported for the two copper complexes of $\text{H}_2\text{do2nph}$, see Table 2. This type of axially elongated distorted octahedral geometry is the most common for cross-bridged cyclen derivatives. Examples are the $[\text{Cu}(\text{cb-do2me})(\text{CH}_3\text{CN})_2]^{2+}$ where the equatorial plane is instead formed by two amines and two MeCN solvent molecules,²⁹ the $[\text{Cu}(\text{cb-do2a})]$ complex in which the equatorial plane is made of two amines and two carboxylate

oxygens,³⁰ or the complex $[\text{Cu}(\text{cb-do2pr})]$ in which the equatorial plane is formed by three amines and one pendant arm oxygen just as found for $[\text{Cu}(\text{cb-do2nph})]$.³¹

Spectroscopic studies

Electronic and EPR spectra. Due to the low solubility in water of the $\text{H}_2\text{do2nph}$ and $\text{H}_2\text{cb-do2nph}$ compounds and especially of their complexes, these studies were performed in DMSO–water (9 : 1, v/v) solution. In Table 3 are compiled the UV-vis as well as the X-band EPR spectroscopic data of the spectra of the copper(II) complexes.

The absorption spectrum at the 500 to 850 nm region of the $[\text{Cu}(\text{do2nph})]$ complex (in its neutral form) shows a band with maximum at 631 nm ($\epsilon = 286 \text{ cm}^{-1} \text{ mol}^{-1} \text{ dm}^3$), which

Table 3 UV-vis and X-band EPR spectroscopic data of the copper(II) complexes of H₂do2nph and H₂cb-do2nph

Complex	UV-vis ^a λ_{\max}/nm ($\epsilon_{\text{molar}}/\text{dm}^3 \text{ mol}^{-1} \text{ cm}^{-1}$)	X-band EPR ^{b,c}					
		g_1	g_2	g_3	A_1^d	A_2^d	A_3^d
[Cu(H ₂ do2nph)] ²⁺	321 (2.1×10^4); 403 (2.1×10^3); 700 (307)	2.215	2.07	2.05	170	14	— ^e
[Cu(Hdo2nph)] ⁺	316 (1.2×10^4); 403 (2.0×10^4); 637 (261)	2.206	2.07	2.04	178	17	— ^e
[Cu(do2nph)]	419 (4.1×10^4); 631 (286)	2.202	2.07	2.04	181	23	— ^e
[Cu(Hcb-do2nph)] ⁺	320 (1.1×10^4); 403 (1.9×10^4); 617 (193)	2.204	2.05	2.04	188	28	— ^e
[Cu(cb-do2nph)]	420 (4.3×10^4); 680 (170)	2.241	2.07	2.04	165	14	10

^a DMSO–H₂O (9 : 1 v/v) solution, recorded at 298 K. ^b In DMSO–H₂O (9 : 1 v/v), recorded at 90 K, microwave power 2.0 mW and frequency (ν) 9.51 GHz. ^c Experimental and simulated EPR spectra are presented in Fig. S1–S5 of the ESI. ^d Values of $A \times 10^4$ in cm^{-1} . ^e Values too low to be accurately determined.

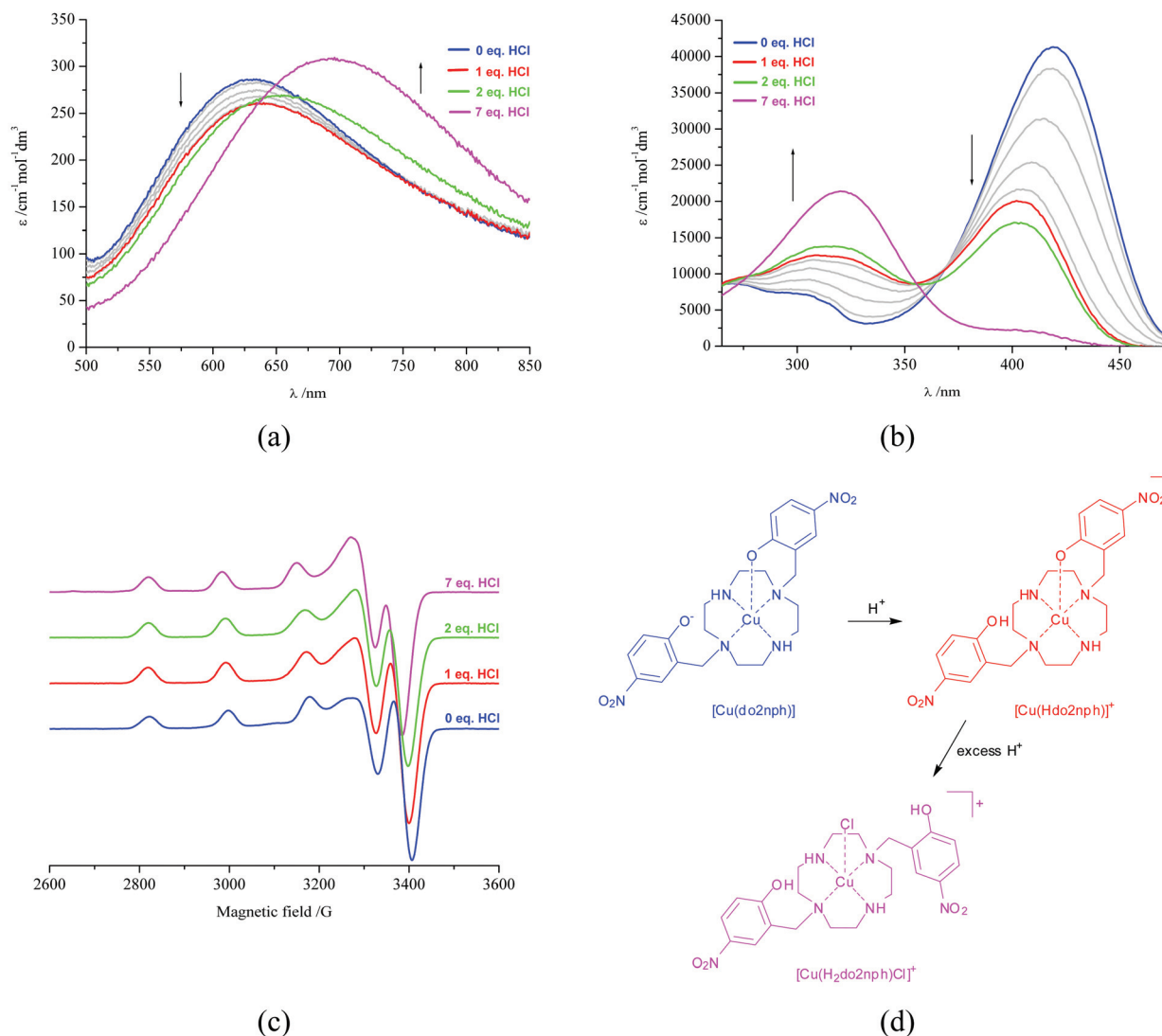


Fig. 5 Spectral changes of the copper(II) complexes of H₂do2nph in DMSO–H₂O (9 : 1 v/v): absorption spectra recorded at 0.0, 0.2, 0.4, 0.6, 0.8, 1.0, 2.0 and 7.0 equiv. of HCl (a) in the 500–850 nm region and (b) in the 265–475 nm region, (c) X-band EPR spectra in frozen solutions, (d) proposed mechanism.

tails into the low-energy region of the spectrum (Fig. 5a, blue spectrum).

The corresponding EPR spectrum (Fig. 5c, blue spectrum) showed one paramagnetic species with the expected four lines at lower field. Simulation of the spectrum indicated three

different principal values for the g parameter of each species, with $g_1 > (g_2 + g_3)/2$ while the lowest g value is ≥ 2.04 , which is characteristic of mononuclear copper(II) complexes in $d_{x^2-y^2}$ ground state and elongation of the axial bonds. Distorted square pyramidal or octahedral stereochemistries are thus

consistent with these data.^{32,33} The position and intensity of the d–d transition band as well as the values of the EPR parameters obtained (see Table 3) are similar to those of copper(II) complexes of cyclen³⁴ and its derivatives bearing one pendant arm, known to possess a distorted square pyramidal geometry.^{35–37} The obtained crystal structure of [Cu(do2nph)] (Fig. 3) also confirms the distorted square pyramidal geometry of the copper centre. Addition of one equivalent of HCl has little effect in the visible absorption and EPR spectra of the complex (Fig. 5a and c), which suggests that its geometry remains essentially the same. The absorption spectra in the 265 to 475 nm region, on the other hand, showed that addition of up to one equivalent of HCl causes a decrease of the band at 419 nm to about half of its height and concomitant increase of a band at 316 nm, with an isosbestic point at 370 nm (Fig. 5b). This behaviour can be attributed to the protonation of one nitrophenolic group of the complex. The fact that protonation of a nitrophenolic arm causes almost no changes in the vis and EPR spectra of the complex suggests that one of the nitrophenolic arms is never coordinated. These observations are also in agreement with the obtained crystal structures of

[Cu(Hdo2nph)]⁺ and [Cu(do2nph)] (Fig. 3), which showed that one of the arms does not coordinate independently of its protonation state, indicating that the structures adopted by these complexes in solution and in the solid state are the same. Addition of another equivalent of HCl causes only slight changes in the spectra of the complex, which means that the second nitrophenolic arm has little tendency to protonate and detach from the metal ion. In fact, complete formation of the [Cu(H₂do2nph)]²⁺ species is achieved only upon addition of 7 equiv. HCl (see Fig. 5).

The copper(II) complexes of H₂cb-do2nph, on the other hand, revealed somewhat different features. The absorption spectrum at the 500 to 850 nm region of the [Cu(do2nph)] complex (in its neutral form) shows a band with maximum at 680 nm ($\epsilon = 170 \text{ cm}^{-1} \text{ mol}^{-1} \text{ dm}^3$), which tails into the low-energy region of the spectrum (Fig. 6a). Simulation of the corresponding EPR spectrum indicated three different principal values for the *g* parameter of each species, with $g_1 > (g_2 + g_3)/2$ with the lowest *g* value being ≥ 2.04 , suggesting distorted square pyramidal or octahedral stereochemistries.^{32,33} The position and low intensity of the d–d transition band as well

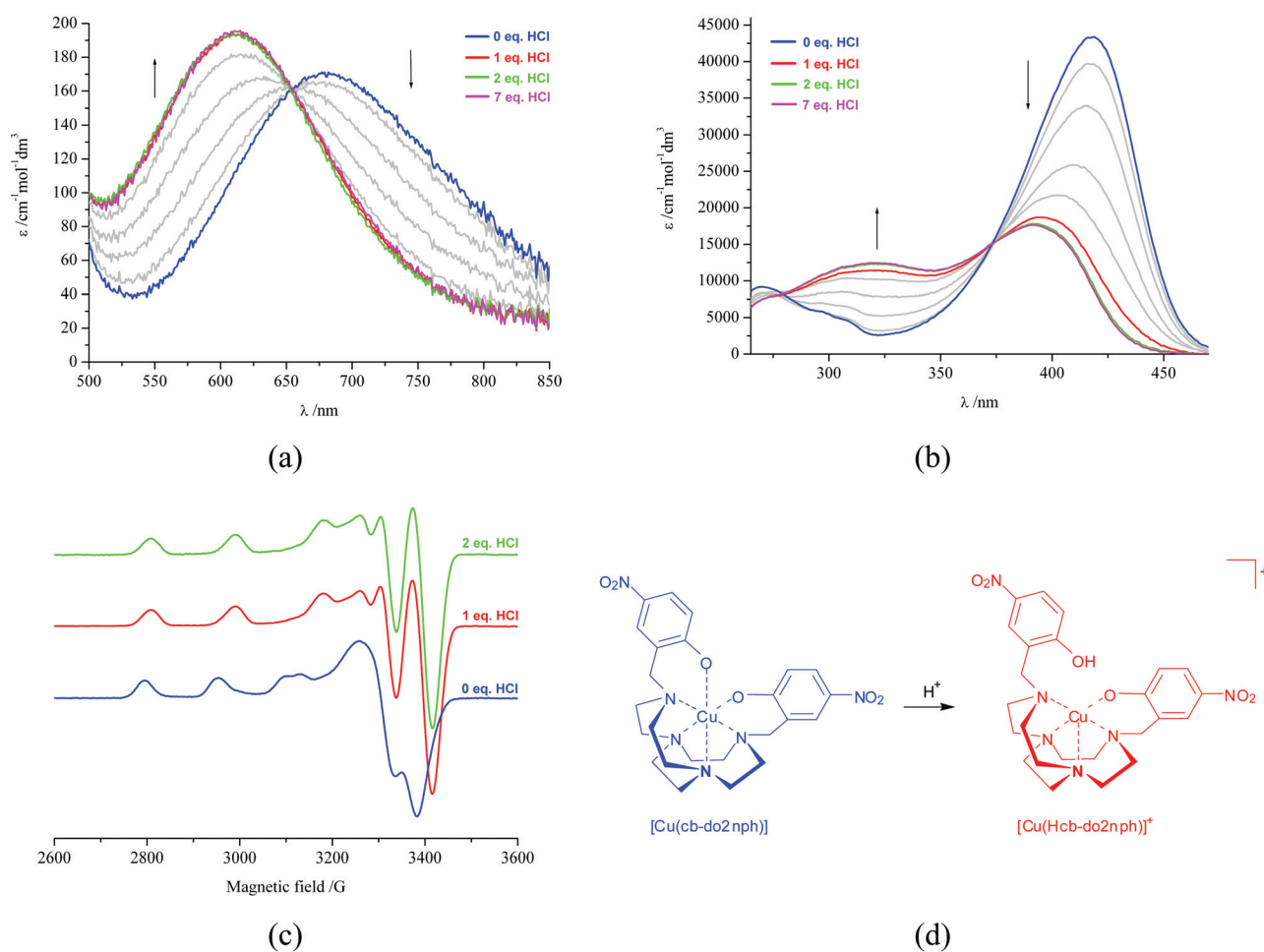


Fig. 6 Spectral changes of the copper(II) complexes of H₂cb-do2nph in DMSO–H₂O (9 : 1 v/v): absorption spectra recorded at 0.0, 0.2, 0.4, 0.6, 0.8, 1.0, 2.0 and 7.0 eq. of HCl (a) in the 500–850 nm region and (b) in the 265–475 nm region, (c) X-band EPR spectra in frozen solutions, (d) proposed mechanism.

as the values of the EPR parameters obtained (see Table 3) are similar to those of copper(II) complexes of cyclen derivatives known to adopt a distorted octahedral geometry.^{28,31,37–39} The crystal structure of [Cu(cb-do2nph)] (Fig. 4) also showed the copper centre in a distorted octahedral geometry. Addition of one equivalent of HCl causes a blue shift of the d–d transition band of 63 nm together with a decrease of the g_1 value and an increase of the A_1 value, consistent with a stronger equatorial ligand field or a weaker axial ligand field, which suggest a change from octahedral to square pyramidal geometry.^{40–42} Addition of up to one equivalent of HCl to the copper(II) complex of the cross-bridged ligand, as also observed for the complex of H₂do2nph, causes a decrease of the band at 418 nm of the absorption spectra to about half of its intensity and a concomitant increase of the band at 320 nm, with an isosbestic point at 373 nm (Fig. 6b). As mentioned above this behaviour can be attributed to the protonation of one nitrophenol group of the complex. Thus, in the case of the H₂cb-do2nph copper(II) complex, the protonation of one nitrophenol arm causes a change from octahedral to square pyramidal geometry consistent with the detachment of one nitrophenol arm from the coordination sphere. Addition of another equivalent of HCl has practically no effect in the spectra of the complex (Fig. 6, green spectra) and further additions of up to 7 equiv. HCl showed no spectral variations, which means that the second nitrophenolic arm has even less tendency to protonate and detach from the metal ion than that in the case of [Cu(Hdo2nph)]. This behaviour is most likely related to the strong coordination interaction of one phenolic oxygen atom on the equatorial plane of the complex as demonstrated by the short Cu–O(25) distance observed in the crystal structure of [Cu(cb-do2nph)] (see Fig. 4 and Table 2).

NMR spectra of the zinc(II) complexes of H₂do2nph and H₂cb-do2nph. The ¹H and ¹³C NMR spectra of the zinc(II) complexes of H₂do2nph and H₂cb-do2nph were recorded in DMSO-d₆ solutions at 298 K, together with 2D correlation spectra to help on the assignment. A single species was found in the spectra of both complexes. The ¹H spectra are reasonably well resolved at room temperature, especially in the region 3–8 ppm where the resonances of the 2-methyl-4-nitrophenol pendant arms appear (see Fig. S6 in the ESI†). A full assignment of these spectra was not attempted due to the complicated resonance pattern at high field, but the involvement of the phenolate pendants in the coordination of zinc(II) could be clearly understood. The ¹H NMR spectrum of [Zn(do2nph)] shows two distinct sets of resonances for the aromatic protons of the pendants, with some overlapping signals. At the same time, the methylene protons of the pendants appear also as two different resonances, one singlet and one quadruplet (AB system). It is thus clear that the two pendant arms are non-equivalent and that only one of them is involved in coordination of the metal cation, see Fig. S6 in the ESI† (top). In contrast, the spectrum of [Zn(cb-do2nph)] showed a single set of resonances for the aromatic protons and only one quadruplet (AB system) for all the methylene protons. This indicates that the pendant arms are magnetically equivalent and both are

coordinated to the metal cation. An inspection of the ¹³C spectra of both complexes (Fig. S7–S8†) showed that a higher symmetry exists in solution for the complex of the cross-bridged ligand compared to the other one. The spectrum of [Zn(cb-do2nph)] has only 12 signals for the 24 carbon nuclei of the ligand backbone, 7 for the two equivalent pendants and 5 for the macrocyclic ring and bridge, indicating an effective C₂ symmetry of the complex in solution. In contrast, the spectrum of [Zn(do2nph)] has a total of 18 signals for the 22 carbon nuclei, 7 for each of the two non-equivalent pendants and another 4 for the macrocyclic ring, pointing to a C₁ symmetry of the complex in solution. Overall, the features found for both zinc(II) complexes suggest their solution structures are similar to the ones found in the solid state for the related copper(II) complexes (see above). Indeed, the spectrum of [Zn(cb-do2nph)] is consistent with a distorted octahedral geometry, while that of [Zn(do2nph)] displays a pentacoordination mode from the ligand alone, which could indicate a square pyramidal geometry.

Kinetic stability of the copper(II) complexes

The kinetics of the acid-assisted dissociation of the copper(II) complexes of both H₂do2nph and H₂cb-do2nph was studied under pseudo-first order conditions in 1 mol dm⁻³ HCl DMSO–H₂O (9 : 1 v/v) solutions at 298.2 K. The dissociation of the complexes was monitored by following the decrease in the visible absorption (700 nm) in the complex of H₂do2nph, or the blue shift of a UV absorption (350 nm) in the complex of H₂cb-do2nph for which the visible absorption is not sufficiently strong in the attainable concentration range. The half-life values found were 10.9 min and 46.1 min for the complexes of H₂do2nph and H₂cb-do2nph, respectively, thus following the expected trend where complexes of cross-bridged ligands are more inert than the complexes of non-bridged parent macrocycles. A few half-life values can be found in the literature for complexes of related cross-bridged cyclen derivatives in 1 mol dm⁻³ HCl aqueous solutions at 303 K, such as 4.0 h for H₂cb-do2a,³⁰ 52.0 min for cb-do2py,²⁸ and 37.2 min for H₂cb-do2pr.³¹ Although these literature values are measured at a slightly higher temperature and for a different solvent than the ones used in our assays, it is still possible to make a rough comparison and conclude that the complex of H₂cb-do2nph exhibits a half-life value for the HCl-assisted dissociation in line with that of other reported cross-bridged derivatives.

Conclusions

Two new cyclen derivatives containing two *trans* 2-methyl-4-nitrophenol pendant arms, H₂do2nph and H₂cb-do2nph, were prepared in good yields and studied comparatively regarding their metal complexation behaviour. Solution and solid state studies revealed that the copper(II) complex of H₂do2nph exhibits a distorted square pyramidal coordination environment with the four nitrogen atoms of the cyclen ring defining the

basal plane and that one of the nitrophenolate arms does not coordinate to the metal, independently of its protonation state. On the other hand, depending on the protonation state of one of the nitrophenolic arms, the cross-bridged derivative forms copper(II) complexes with distorted square pyramidal or octahedral geometries with one or two arms coordinated to the metal centre, respectively. In the complex with distorted octahedral geometry, the two phenolic oxygen atoms are coordinated to the metal centre in a *cis*-fashion. ^1H and ^{13}C NMR spectra of the zinc(II) complexes of both ligands showed identical features, pointing also to a distorted square pyramidal coordination environment in $[\text{Zn}(\text{do2nph})]$ and an octahedral geometry in $[\text{Zn}(\text{cb-do2nph})]$. Overall, we could have a clear insight of the coordination properties of copper(II) and zinc(II) complexes of both ligands in solution. Furthermore, the structures found in solution correlate well with those determined in the solid state. Despite the unusual solution medium used in the acid-assisted dissociation assays, the half-life found for the copper(II) complex of $\text{H}_2\text{cb-do2nph}$ shows that it is quite inert when compared to other cross-bridged cyclen derivatives.

It is known from the literature that copper(II) complexes of cyclen derivatives with two or more coordinating pendant arms may exhibit square pyramidal as well as octahedral geometries, with the preference being dictated by the type and length of the pendant groups, while the complexes of cross-bridged cyclen derivatives adopt most frequently distorted octahedral geometries, although square pyramidal environments cannot be discarded as seen in the present work. Here, we have demonstrated that two phenolic arms appended on cyclen derivatives resulted in chelators with a good coordination ability for copper(II) and zinc(II) metal ions, especially the cross-bridged derivative where an octahedral geometry is preferred. The use of such a chelate structure may prove very interesting for metal radioisotopes used in medical applications, provided that changes are made on the ligand structure in order to increase the solubility of the complexes in aqueous media. Envisaged radioisotopes are not only those of copper(II), but possibly also those of gallium(III) which have identical ionic radii and invariably adopt octahedral geometry. The nitro groups present in the ligands can be easily transformed in order to increase solubility and also to bind a biomolecule for use in targeted medical applications. We are currently developing modified ligands with the above aims, and the promising properties already observed for their complexes will be disclosed in due time.

Experimental

General considerations

Cyclen-glyoxal was prepared by adaptation of a literature procedure.⁴³ All solvents and chemicals were commercially purchased with reagent grade quality and used as supplied without further purification. NMR spectra were recorded on a Bruker Avance II+ 400 MHz instrument. Peak assignments are based on peak integration and multiplicity for 1D ^1H spectra and on

2D HMQC experiments (Fig. S9–S18 in the ESI†). Microanalyses were carried out by the ITQB/IBET Analytical Services Unit. The electronic absorption spectra were recorded on a UNICAM UV-vis spectrophotometer model UV-4. EPR spectra were recorded on a Bruker EMX 300 spectrometer equipped with continuous-flow cryostat for liquid nitrogen, operating at the X-band.

Syntheses

Cyclen-glyoxal *trans*-bis(2-methyl-4-nitrophenol) diammonium bromide. A solution of 2-(bromomethyl)-4-nitrophenol (1.363 g, 5.9 mmol) in MeCN (10 cm³) was added dropwise over 30 min to a stirred solution of cyclen-glyoxal (0.456 g, 2.4 mmol) in MeCN (10 cm³). The solution was left under stirring at r.t. for 8 days, during which time a white precipitate formed. The solid was filtered, washed with MeCN and then with diethyl ether. The compound was vacuum dried and found pure (1.483 g, 96%); m.p. 225 °C (decomp.). ^1H NMR (400 MHz, DMSO-*d*₆): δ 8.57 (2 H, d, $J = 2.8$ Hz, 3-H), 8.32 (2 H, dd, $J = 9.0, 2.8$ Hz, 5-H), 7.20 (2 H, d, $J = 9.0$ Hz, 6-H), 4.95, 4.74 (4 H, ABq, $J_{\text{AB}} = 13$ Hz, CH_2nph) 4.75 (2 H, s, *CH*-bisaminal), 4.18–2.88 (16 H, m, CH_2 -ring) ppm. ^{13}C NMR (100 MHz, DMSO-*d*₆): δ 163.9 (C4), 140.0 (C1), 131.5 (C3), 128.6 (C6), 117.3 (C2), 115.1 (C5), 77.2 (*CH*-bisaminal), 60.0 (CH_2nph), 56.8, 54.8, 46.5, 43.1 (C-ring) ppm.

$\text{H}_2\text{do2nph}$ hydrochloride. The diammonium bromide from above (1 g, 1.5 mmol) was suspended in a solution of hydrazine monohydrate–water 1 : 1 v/v (13 cm³) and refluxed for 2 h. The mixture was allowed cooled to r.t. and a yellow precipitate formed which was filtered, washed with water and then with diethyl ether. This solid was recrystallised from boiling HCl–EtOH (1 : 1 v/v), yielding a white crystalline solid which was dried in an oven at 60 °C (0.908 g, 91%); m.p. 250 °C (decomp.). ^1H NMR (400 MHz, D₂O) δ 8.18 (2 H, dd, $J = 8.9, 2.8$ Hz, 5-H), 8.15 (2 H, d, $J = 2.8$ Hz, 3-H), 7.00 (2 H, d, $J = 8.9$ Hz, 6-H), 3.68 (4 H, s, CH_2nph), 3.68–2.87 (16H, $\text{NHCH}_2\text{CH}_2\text{N}$) ppm. ^{13}C NMR (100 MHz, D₂O): δ 161.6 (C4), 140.4 (C1), 128.2 (C3), 126.4 (C6), 123.3 (C2), 116.1 (C5), 51.5 (CH_2nph), 47.4 (NHCH_2), 42.5 (CH_2N) ppm. Anal. calcd. for $\text{C}_{22}\text{H}_{30}\text{N}_6\text{O}_6 \cdot 5\text{HCl}$: C, 40.3; H, 5.4; N, 12.8%. Found: C, 40.8; H, 5.2; N, 12.3%. ESI-MS (H_2O –MeOH, 8 : 2) m/z : 475.0 [$\text{M} + \text{H}$]⁺.

$\text{H}_2\text{cb-do2nph}$ hydrochloride. The diammonium bromide from above (1.490 g, 2.3 mmol) was suspended in EtOH–H₂O 95 : 5 (150 cm³) and solid NaBH_4 (0.855 g, 22 mmol) was added in small portions. The mixture was left under stirring at r.t. for 8 days, then cooled in an ice bath, acidified with 2 mol dm^{−3} HCl and left stirring for another 2 h. The precipitate thus formed was filtered, washed with EtOH and then with diethyl ether, and dried in an oven at 60 °C (1.422 g, 92%). M.p. 163–164 °C. ^1H NMR (400 MHz, D₂O) δ 8.30 (2 H, d, $J = 2.8$ Hz, 3-H), 8.24 (2 H, dd, $J = 9.0, 2.8$ Hz, 5-H), 7.11 (2 H, d, $J = 9.0$ Hz, 6-H), 4.38 (4 H, s, CH_2nph), 3.60–3.10 (16 H, $\text{NCH}_2\text{CH}_2\text{N}$ -ring), 3.20 (4 H, s, $\text{NCH}_2\text{CH}_2\text{N}$ -bridge) ppm. ^{13}C NMR (100 MHz, D₂O): δ 161.9 (C4), 140.4 (C1), 128.2 (C3), 127.3 (C5), 120.4 (C2), 116.2 (C6), 54.3 (CH_2nph), 54.2, 53.9 (CH_2 -ring), 46.7 (CH_2 -bridge) ppm. Anal. calcd for

$C_{24}H_{32}N_6O_6 \cdot 5HCl$: C, 42.2; H, 5.5; N, 12.3%. Found: C, 42.2; H, 5.6; N, 12.3%. ESI-MS (H_2O -MeOH, 8 : 2) m/z : 501.1 $[M + H]^+$.

[Cu(do2nph)]. The compound $H_2do2nph$ (99 mg, 151 μ mol) was dissolved in MeOH- H_2O 1 : 1 v/v (50 cm^3), 0.95 equiv. of $Cu(ClO_4)_2$ was added, pH was rendered basic with aqueous KOH and the dark green solution was heated at 60 °C for 3 h. After cooling to r.t. the pH was neutral and the MeOH was removed on a rotary evaporator. A crystalline dark green solid precipitated as the mixture cooled to r.t. The solid was filtered, washed with cold water and dried in an oven at 60 °C until constant mass (70 mg, 90.3%). Anal. calcd. for $C_{22}H_{28}CuN_6O_6$: C, 49.5; H, 4.9; N, 15.7%. Found: C, 49.1; H, 5.2; N, 15.6%.

[Cu(cb-do2nph)]. A procedure similar to the one described for [Cu(do2nph)] was used for $H_2cb-do2nph$ (100 mg, 146 μ mol), producing a fine green powder (70 mg, 89.9). Anal. calcd. for $C_{24}H_{30}CuN_6O_6$: C, 51.3; H, 5.4; N, 15.0%. Found: C, 51.3; H, 5.3; N, 14.6%.

[Zn(do2nph)]. The compound $H_2do2nph$ (62 mg, 94 μ mol) was dissolved in MeOH (20 cm^3), and 0.95 equiv. of $ZnCl_2$ was dissolved in water (20 mL) and added to the $H_2do2nph$ solution. The pH was rendered basic with aqueous KOH, the solution turned yellow and after 5 min stirring a precipitate with the same colour appeared. The mixture was heated at 70 °C during 2 days, cooled until r.t. and pH was checked as neutral. Upon removal of MeOH on a rotary evaporator a light yellow powder precipitated. The solid was filtered, washed with water and diethyl ether, and dried in an oven at 60 °C until constant mass (47 mg, 97.4%). Anal. calcd for $C_{22}H_{28}ZnN_6O_6$: C, 49.1; H, 5.3; N, 15.6%. Found: C, 49.2; H, 5.0; N, 15.6%. 1H NMR (400 MHz, D_2O) δ 2.2–3.3 (16 H, m, ring CH_2), 3.65 (2 H, s, uncoordinated pendant CH_2), 3.87, 4.16 (2 H, ABq, $J_{AB} = 12.6$ Hz, coordinated pendant CH_2), 6.25, 7.85 (2 \times 1 H, d, coordinated pendant aromatics), 6.40 (1 H, d, uncoordinated pendant aromatic), 7.90 (3 H, m, mixed aromatics) ppm. ^{13}C NMR (100 MHz, D_2O): δ 44.0, 45.0 (2 \times 1 C, ring CH_2), 44.5, 51.7 (2 \times 3 C, ring CH_2), 56.8 (1 C, uncoordinated pendant CH_2), 61.1 (1 C, coordinated pendant CH_2), 119.8 (2 C, aromatic CH_2), 122.5, 123.8, 126.4, 126.5, 127.4, 128.4, 131.5, 131.7, 176.0, 176.9 (10 \times 1 C, aromatic CH_2) ppm.

[Zn(cb-do2nph)]. A procedure similar to the one described for [Zn(do2nph)] was used for $H_2cb-do2nph$ (62 mg, 91 μ mol), producing a fine yellow powder (46 mg, 99.1%). Anal. calcd for $C_{24}H_{30}ZnN_6O_6$: C, 51.1; H, 5.4; N, 14.9%. Found: C, 51.3; H, 5.1; N, 15.5%. 1H NMR (400 MHz, D_2O) δ 2.2–3.3 (16 H, m, ring CH_2), 3.83, 4.41 (4 H, ABq, $J_{AB} = 12.2$ Hz, coordinated pendants CH_2), 6.35, 7.91, 8.00 (3 \times 1 H, d, coordinated pendants aromatics) ppm. ^{13}C NMR (100 MHz, D_2O): δ 49.4, 55.2, 57.3, 57.7, 58.5 (5 \times 2 C, ring and bridge CH_2), 61.8 (2 C, pendants CH_2), 119.4, 123.0, 126.8, 129.0, 132.4, 176.4 (6 \times 2 C, aromatic CH_2) ppm.

Crystals of $H_4do2nph$. About 2 μ mol of $H_4do2nph$ hydrochloride was dissolved in the minimum amount of MeOH- H_2O (1 : 1 v/v). The solution was allowed to evaporate slowly at r.t. Yellow single crystals grew within a week.

Crystals of $H_2cb-do2nph$. About 2 μ mol of $H_2cb-do2nph$ hydrochloride was dissolved in the minimum amount of H_2O and aqueous KOH was added up to neutral pH. MeOH was

then added to approximately 1 : 1 v/v and the solution was allowed to evaporate slowly at r.t. Yellow single crystals were obtained within two weeks.

Crystals of [Cu(do2nph)]. To 1 cm^3 of a 2×10^{-3} mol dm^{-3} solution of $H_2do2nph$ in MeOH- H_2O (1 : 1 v/v) was added 1 equiv. of an aqueous $Cu(ClO_4)_2$ solution. Aqueous KOH was added to neutral pH and the solution heated to 60 °C for 1 h. After cooling to r.t. the pH was readjusted to neutral and the solution was allowed to evaporate slowly at r.t. Blue single crystals grew in one week.

Crystals of [Cu(cb-do2nph)]. Procedure similar to the one for [Cu(do2nph)]. After a week two types of crystals formed: green and blue coloured crystals.

Crystals of [Zn(cb-do2nph)]. Procedure similar to the one for [Cu(do2nph)]. After a week yellow crystals formed.

Spectroscopic studies

UV-vis spectra were measured at 298 K in DMSO- H_2O (9 : 1 v/v) solutions. Concentrations in the vis region were of 5.5×10^{-4} mol dm^{-3} for [Cu(do2nph)] and of 3.47×10^{-4} mol dm^{-3} for [Cu(cb-do2nph)], while in the UV region they were 1.80×10^{-5} mol dm^{-3} in both cases. Aliquots of diluted HCl were added to these solutions until 7 equivalents of acid was present. The solutions used to measure the vis spectra were frozen (90 K) and used as they were to acquire EPR spectra. X-band EPR spectroscopic measurements of the copper(II) complexes were recorded at microwave power 2.0 mW and frequency (ν) 9.51 GHz. EPR spectra were simulated with the SpinCount software⁴⁴ to obtain the relevant parameters. NMR samples of the zinc(II) complexes were prepared in DMSO- d_6 at ca. 1.0×10^{-2} mol dm^{-3} . 1H , ^{13}C , COSY, NOESY and HMQC spectra were run at 298 K with the chemical shifts referenced to the solvent residual peak ($\delta = 2.50$ ppm on 1H and $\delta = 39.52$ ppm on ^{13}C).

Kinetic inertness of the copper(II) complexes

The acid-assisted dissociation of the complexes of both ligands with copper(II) was studied in 1 mol dm^{-3} HCl under pseudo-first order conditions by addition of concentrated aqueous solutions of HCl to solutions of the preformed complexes in DMSO, while keeping the final solutions at 9 : 1 (v/v) in DMSO- H_2O . Dissociation experiments were performed at 298.2 K by following the spectral absorption bands of the complexes in the vis ($H_2do2nph$) or UV ($H_2cb-do2nph$) range at 700 nm and 350 nm, respectively. The concentration of the complexes in the experiments was at 5.3×10^{-4} mol dm^{-3} for $H_2do2nph$ or 2.4×10^{-5} mol dm^{-3} for $H_2cb-do2nph$, without any control of the ionic strength. Experimental data were processed by exponential regression in order to calculate the half-lives from the fitting equation.

Crystallography

The single crystal X-ray data of $[H_4do2nph](ClO_4)_2 \cdot 2H_2O$ 1, $H_2cb-do2nph \cdot 1.5H_2O$ 2, $[Cu(do2nph)][Cu(Hdo2nph)]ClO_4 \cdot 3H_2O$ 3, and $[Cu(cb-do2nph)] \cdot H_2O$ 4 were collected on a CCD Bruker APEX II at 150(2) K using graphite monochromatized Mo-K α radiation ($\lambda = 0.71073$ Å). The selected crystal of each

Table 4 Crystal data and selected refinement details for the H₂do2nph and H₂cb-do2nph compounds and their copper(II) complexes

Compound	[H ₄ do2nph](ClO ₄) ₂ ·H ₂ O 1	[H ₂ cb-do2nph]·1.5H ₂ O 2	[Cu(do2nph)][Cu(Hdo2nph)]ClO ₄ ·3H ₂ O 3	[Cu(cb-do2nph)]·H ₂ O 4
Empirical Formula	C ₂₂ H ₃₆ Cl ₂ N ₆ O ₁₆	C ₂₄ H ₃₅ N ₆ O _{7.50}	C ₄₄ H ₅₉ ClCu ₂ N ₁₂ O ₁₉	C ₂₄ H ₃₂ CuN ₆ O ₇
<i>M_w</i>	711.47	532.08	1222.56	580.10
Crystal system	Triclinic	Tetragonal	Monoclinic	Monoclinic
Space group	<i>P</i> 1	<i>P</i> 4 ₂ <i>c</i>	<i>Cc</i>	<i>Cc</i>
<i>a</i> /[Å]	8.6397(3)	16.7755(5)	21.9871(7)	23.2324(10)
<i>b</i> /[Å]	9.7922(4)	16.7755(5)	16.3897(3)	10.1166(5)
<i>c</i> /[Å]	18.6551(9)	17.8638(7)	16.9181(5)	12.6511(6)
<i>α</i> /[°]	100.664(3)	(90)	(90)	(90)
<i>β</i> /[°]	99.990(3)	(90)	119.432(1)	122.370(2)
<i>γ</i> /[°]	100.033(2)	(90)	(90)	90
<i>V</i> /[Å ³]	1492.37(11)	5027.2(3)	5309.8(3)	2511.4(2)
<i>Z</i>	2	8	4	4
<i>D_c</i> [Mg m ⁻³]	1.583	1.394	1.534	1.534
<i>μ</i> /[mm ⁻¹]	0.304	0.105	0.937	0.927
Reflections collected	23 591	64 273	25 343	22 481
Unique reflections	8974 [0.0215]	6773 [0.0413]	12 168 [0.0500]	7236 [0.0452]
[<i>R</i> _{int}]				
Final <i>R</i> indices				
<i>R</i> ₁ , <i>wR</i> ₂ [<i>I</i> > 2σ(<i>I</i>)]	0.0505, 0.1532 [6963]	0.0622, 0.1732 [5881]	0.0690, 0.1544 [9816]	0.0550, 0.1540 [6325]
<i>R</i> ₁ , <i>wR</i> ₂ (all data)	0.0702, 0.1864	0.0724, 0.1835	0.0934, 0.1946	0.0664, 0.1680

compound was positioned at 35 mm from the CCD. The diffraction spots were measured with a counting time of 40 s for **4** and 60 s for remaining compounds. Data reduction of each compound comprising a multi-scan absorption correction was carried out using the SAINT-NT from Bruker AXS. The structures were solved with SHELXS by direct methods and refined on *F*² using full-matrix least squares with SHELXL available from the SHELX-97 package.⁴⁵ The X-ray diffraction pattern of **3** was consistent with space groups *Cc* and *C2/c*. The structure was solved in both space groups, but the structure refinement was only successful in the non-centrosymmetric one. All non-hydrogen atoms were refined with anisotropic thermal parameters. C–H hydrogen atoms were introduced at calculated positions and refined with *U*_{iso} = 1.2*U*_{eq} of the parent atom. In the crystal structures of **1** and **3**, the ClO₄[−] counter-ion was found disordered over two tetrahedral positions which were included in the structure refinement with refined occupancies of *x* and 1 − *x*, being *x* equal to 0.538(4) and 0.69(2), respectively. The macrocyclic backbone of **2**, showed one ethane linkage disordered over two positions, which were refined with statistical occupancies of 0.63(1) and 0.37(1), respectively. The atomic positions of −NH₂ groups of **1** were obtained from the last difference Fourier maps and were refined with individual isotropic temperature factors as well as the N–H hydrogen atom of **2**. The atomic coordinates of the hydrogen atoms of each phenol group of this compound were also revealed by the last Fourier maps while the hydrogen atom of the single phenol group was introduced *via* AFIX 147 command using the initial coordinates of the hydrogen corresponding to the trial position determined by the maximum number of hydrogen bonds established in crystal packing with neighbouring molecules namely crystallisation water molecules. The atomic positions of the hydrogen atoms of the crystallisation water molecules with entire occupancy were obtained from last difference Fourier maps with exception for **2** and **4**, which

were not revealed. All O–H hydrogen atoms were refined with isotropic thermal constraint of *U*_{iso} = 1.2*U*_{eq}. The hydrogen atoms of the disordered water molecules or half occupancy were not taken into account in the structure refinement. Final *R* values together with pertinent crystallographic data are summarized in Table 4 for the H₂do2nph and H₂cb-do2nph compounds and their metal complexes. ORTEP diagrams were drawn with Ortep-3 for windows,⁴⁶ and the representation of [H₄do2nph]²⁺ in stick fashion was obtained with Pymol.⁴⁷

Acknowledgements

The authors acknowledge Fundação para a Ciência e a Tecnologia (FCT), with co-participation of the European Community funds FEDER, POCI, QREN and COMPETE, for the financial support and the fellowship of C. V. Esteves under project PTDC/QUI/67175/2006. P. Mateus and L. M. P. Lima acknowledge FCT also for the postdoctoral fellowships SFRH/BPD/79518/2011 and SFRH/BPD/73361/2010, respectively. The NMR spectrometers are part of the National NMR Network and were purchased in the framework of the National Program for Scientific Re-equipment, contract REDE/1517/RMN/2005, with funds from POCI 2010 (FEDER) and FCT. We also acknowledge M. C. Almeida for providing elemental analysis and ESI-MS data from the ITQB/IBET Analytical Services Unit.

References

- 1 R. Delgado, V. Félix, L. M. P. Lima and D. W. Price, *Dalton Trans.*, 2007, 2734–2743.
- 2 R. E. Mewis and S. J. Archibald, *Coord. Chem. Rev.*, 2010, **254**, 1686–1712.

- 3 P. Hermann, J. Kotek, V. Kubiček and I. Lukeš, *Dalton Trans.*, 2009, 3027–3047.
- 4 T. J. Wadas, E. H. Wong, G. R. Weisman and C. J. Anderson, *Chem. Rev.*, 2010, **110**, 2858–2902.
- 5 S. Bhattacharyya and M. Dixit, *Dalton Trans.*, 2011, 6112–6128.
- 6 M. Shokeen and C. J. Anderson, *Acc. Chem. Res.*, 2009, **42**, 832–841.
- 7 M. Woods, G. E. Kiefer, S. Bott, A. Castillo-Muzquiz, C. Eshelbrenner, L. Michaudet, K. McMillan, S. D. K. Mudigunda, D. Ogrin, G. Tirso, S. Zhang, P. Zhao and A. D. Sherry, *J. Am. Chem. Soc.*, 2004, **126**, 9248–9256.
- 8 P. Dapporto, V. Fusi, M. Micheloni, P. Palma, P. Paoli and R. Pontellini, *Inorg. Chim. Acta*, 1998, **275–276**, 168–174.
- 9 G. Ambrosi, M. Formica, V. Fusi, L. Giorgi and M. Micheloni, *Coord. Chem. Rev.*, 2008, **252**, 1121–1152.
- 10 E. Kimura, T. Koike and M. Takahashi, *J. Chem. Soc., Chem. Commun.*, 1985, 385–386.
- 11 Y. Iitaka, T. Koike and E. Kimura, *Inorg. Chem.*, 1986, **25**, 404–405.
- 12 E. Kimura, M. Yamaoka, M. Morioka and T. Koike, *Inorg. Chem.*, 1986, **25**, 3883–3886.
- 13 E. Kimura, S. Joko, T. Koike and M. Kodama, *J. Am. Chem. Soc.*, 1987, **109**, 5528–5529.
- 14 E. Kimura, T. Koike, K. Uenishi, M. Hediger, M. Kuramoto, S. Joko, Y. Arai, M. Kodama and Y. Iitaka, *Inorg. Chem.*, 1987, **26**, 2975–2983.
- 15 E. Kimura, T. Koike and K. Toriumii, *Inorg. Chem.*, 1988, **27**, 3687–3688.
- 16 D. A. Moore, P. E. Fanwick and M. J. Welch, *Inorg. Chem.*, 1989, **28**, 1504–1506.
- 17 D. A. Moore, P. E. Fanwick and M. J. Welch, *Inorg. Chem.*, 1990, **29**, 612–616.
- 18 U. Auerbach, U. Eckert, K. Wieghardt, B. Nuber and J. Weiss, *Inorg. Chem.*, 1990, **29**, 938–944.
- 19 U. Auerbach, T. Weyhermüller, K. Wieghardt, B. Nuber, E. Bill, C. Butzlaff and A. X. Trautwein, *Inorg. Chem.*, 1993, **32**, 508–519.
- 20 J. Rohovec, R. Gyepes, I. Císařová, J. Rudovský and I. Lukeš, *Tetrahedron Lett.*, 2000, **41**, 1249–1253.
- 21 G. Hervé, H. Bernard, N. Le Bris, M. Le Baccon, J.-J. Yaouanc and H. Handel, *Tetrahedron Lett.*, 1999, **40**, 2517–2520.
- 22 G. R. Weisman, E. H. Wong, D. C. Hill, M. E. Rogers, D. P. Reed and C. Calabrese, *Chem. Commun.*, 1996, 947–948.
- 23 P. Dapporto, V. Fusi, C. Giorgi, M. Micheloni, P. Palma, P. Paoli and R. Pontellini, *Supramol. Chem.*, 1999, **10**, 243–252.
- 24 A. W. Addison, T. N. Rao, J. Reedijk, J. van Rijn and G. C. Verschoor, *J. Chem. Soc., Dalton Trans.*, 1984, 1349–1356.
- 25 R. Clay, P. Murray-Rust and J. Murray-Rust, *Acta Crystallogr., Sect. B: Struct. Sci.*, 1979, **35**, 1894–1895.
- 26 A. Riesen, M. Zehnder and T. A. Kaden, *J. Chem. Soc., Chem. Commun.*, 1985, 1336–1338.
- 27 A. Riesen, M. Zehnder and T. A. Kaden, *Helv. Chim. Acta*, 1986, **69**, 2074–2080.
- 28 N. Bernier, J. Costa, R. Delgado, V. Félix, G. Royal and R. Tripier, *Dalton Trans.*, 2011, **40**, 4514–4526.
- 29 T. J. Hubin, N. W. Alcock, M. D. Morton and D. H. Busch, *Inorg. Chim. Acta*, 2003, **348**, 33–40.
- 30 C. A. Boswell, X. Sun, W. Niu, G. R. Weisman, E. H. Wong, A. L. Rheingold and C. J. Anderson, *J. Med. Chem.*, 2004, **47**, 1465–1474.
- 31 K. J. Heroux, K. S. Woodin, D. J. Tranchemontagne, P. C. B. Widger, E. Southwick, E. H. Wong, G. R. Weisman, S. A. Tomellini, T. J. Wadas, C. J. Anderson, S. Kassel, J. A. Golend and A. L. Rheingold, *Dalton Trans.*, 2007, 2150–2162.
- 32 B. J. Hathaway and D. E. Billing, *Coord. Chem. Rev.*, 1970, **5**, 143–207.
- 33 B. J. Hathaway, *Coord. Chem. Rev.*, 1983, **52**, 87–169.
- 34 M. C. Styka, R. C. Smierciak, E. L. Blinn, R. E. DeSimone and J. V. Passariello, *Inorg. Chem.*, 1978, **17**, 82–86.
- 35 S. E. Ghachtouli, C. Cadiou, I. Déchamps-Olivier, F. Chuburu, M. Aplincourt and T. Roisnel, *Eur. J. Inorg. Chem.*, 2006, 3472–3481.
- 36 S. Lacerda, M. P. Campello, I. C. Santos, I. Santos and R. Delgado, *Polyhedron*, 2007, **26**, 3763–3773.
- 37 A. E. Majzoub, C. Cadiou, I. Déchamps-Olivier, F. Chuburu, M. Aplincourt and B. Tinant, *Inorg. Chim. Acta*, 2009, **362**, 1169–1178.
- 38 P. Barbaro, C. Bianchini, G. Capannesi, L. Di Luca, F. Laschi, D. Petroni, P. A. Salvadori, A. Vacca and F. Vizza, *J. Chem. Soc., Dalton Trans.*, 2000, 2393–2401.
- 39 C. F. G. C. Geraldes, M. P. M. Marques, B. De Castro and E. Pereira, *Eur. J. Inorg. Chem.*, 2000, 559–565.
- 40 R. P. Bonomo, F. Riggi and A. J. Di Bilio, *Inorg. Chem.*, 1988, **27**, 2510–2512.
- 41 M. Valko, H. Morris, M. Mazúr, J. Telser, E. J. L. McInnes and F. E. Mabbs, *J. Phys. Chem. B*, 1999, **103**, 5591–5597.
- 42 N. Niklas and R. Alsfasser, *Dalton Trans.*, 2006, 3188–3199.
- 43 M. Le Baccon, F. Chuburu, L. Toupet, H. Händel, M. Soibinet, I. Déchamps-Olivier, J.-P. Barbier and M. Aplincourt, *New J. Chem.*, 2001, **25**, 1168–1174.
- 44 SpinCount is a Windows software package that allows quantitative interpretation and simulation of EPR spectra, created by Prof. M. P. Hendrich at Carnegie Mellon University. SpinCount is available at <http://www.chem.cmu.edu/groups/hendrich/>
- 45 G. M. Sheldrick, *Acta Crystallogr., Sect. A: Fundam. Crystallogr.*, 2008, **64**, 112.
- 46 L. J. Farrugia, *J. Appl. Crystallogr.*, 1997, **30**, 565.
- 47 *The PyMOL Molecular Graphics System, Version 1.2r3pre*, Schrödinger, LLC.